EUROFUSION WPJET3-PR(14) 12700

P Batistoni et al.

Benchmark experiments on neutron streaming (Endorser X. Litaudon)

Preprint of Paper to be submitted for publication in
Nuclear Fusion

This work has been carried out within the framework of the EUROfusion Consortium and has received funding from the Euratom research and training programme 2014-2018 under grant agreement No 633053. The views and opinions expressed herein do not necessarily reflect those of the European Commission.

Benchmark experiments on neutron streaming through JET Torus Hall penetrations

P. Batistoni[1], S. Conroy[2], S. Lilley[3], J. Naish[3], B. Obryk[4], S. Popovichev[3], I. Stamatelatos[5], B. Syme[3] and T. Vasilopoulou[5]

[1] ENEA - Fusion Technical Unit, Via E. Fermi, 45, I-00044 Frascati (Rome), Italy
[2] Uppsala University, Box 516, 751 20 Uppsala, Sweden
[3]CCFE, Culham Science Centre, Abingdon, Oxfordshire, OX14 3DB United Kingdom
[4] Institute of Nuclear Physics, ul. Radzikowskiego 152, 31-342 Kraków, Poland
[5] Institute of Nuclear and Radiological Sciences, Energy, Technology and Safety, National Centre for Scientific Research "Demokritos, Athens, Greece

Abstract

Neutronics experiments are performed at JET for validating in a real fusion environment the neutronics codes and nuclear data applied in ITER nuclear analyses. In particular, the neutron fluence through the penetrations of the JET torus hall is measured and compared with calculations to assess the capability of state-of-art numerical tools to correctly predict the radiation streaming in the ITER biological shield penetrations up to large distances from the neutron source, in large and complex geometries.

Neutron streaming experiments started in 2012 when several hundreds of very sensitive thermo-luminescence detectors (TLD), enriched to different levels in ^{6}LiF/^{7}LiF, were used to measure the neutron and gamma dose separately. Lessons learnt from this first experiment led to significant improvements in the experimental arrangements to reduce the effects due to directional neutron source and self-shielding of TLDs. Here we report the results of measurements performed during the 2013-2014 JET campaign. Data from new positions, at further locations in the South West labyrinth and down to the Torus Hall basement through the air duct chimney, were obtained up to about 60 m distance from the plasma neutron source. In order to avoid interference between TLDs due to self-shielding effects, only TLDs containing natural Lithium and 99.97% ^{7}Li were used. All TLDs were located in the centre of large Polyethylene (PE) moderators, with ^{nat}Li and ^{7}Li crystals evenly arranged within two PE containers, one in horizontal and the other in vertical orientation, to investigate the shadowing effect in the directional neutron field. All TLDs were calibrated in the quantities of air kerma and neutron fluence. This improved experimental arrangement led to reduced statistical spread in the experimental data.

The MCNP Monte Carlo N-Particle code was used to calculate the air kerma due to neutrons and the neutron fluence at detector positions, using a JET model validated up to the magnetic limbs. JET biological shield and penetrations, the PE moderators and TLDs were modeled in detail. Different tallying methods were used in the calculations, which are routinely used in ITER nuclear analyses: the mesh tally and the track length estimator with multiple steps calculations using the Surface Source Write /Read capability available in MCNP. In both cases, the calculated neutron fluence (C) was compared to the measured fluence (E) and hence C/E comparisons have been obtained and are discussed.

1. Introduction

The evaluation of neutron streaming through the ITER machine penetrations and through ducts in the biological shields is a major safety task involving detailed computation, using state-of-the-art radiation transport codes, of long paths and in complex geometries. The effect results from a large number of scattering collisions of neutrons in the forward direction along the streaming path walls, as well as from neutron attenuation by the shielding structures. So, the correct evaluation of neutron streaming through long distances requires the availability of accurate angle-energy double differential neutron cross sections as well as powerful numerical tools capable of handling large and complex volumes, and to produce statistically meaningful results.

JET is the largest operating fusion device, which produces neutron emission rates in excess of 10^{16} n/s in DD operations. A new DT campaign is also foreseen in 2017 with neutron emission rates in excess of 10^{18} n/s and a total neutron yield up to 1.7 x 10^{21} neutrons.

In the frame of a wide technological program, several neutronics experiments are carried out at JET which aim to validate the numerical tools used for neutron calculations in ITER design in real a fusion environment [1].

In particular, neutron streaming experiments are carried out at JET using very sensitive thermoluminescence detectors (TLD) which allow one to measure the neutron /gamma ray dose (air kerma) and the neutron fluence at distant positions from the machine, up to several tens of meters, outside the Torus Hall biological shield. No other neutron detector could be suitable for this application. TLDs are well developed technology in the field of passive radiation sensors. Among them, lithium fluoride MCP (LiF:Mg,Cu,P) detectors present very high sensitivity and a simple signal to dose relation, and allow to measure doses ranging from micrograys up to a megagray [2 - 4]. These TLDs were already used in a first benchmark experiment carried out at JET in 2012 [5] when they were used to derive the neutron fluence in eleven different positions inside the JET Torus Hall and along its penetrations, namely the South West (SW) labyrinth and the South East (SE) chimney where large air ducts are located. The experiment was simulated by neutronics calculations using the MCNP Monte Carlo N-Particle code [6] and the available model of JET device and Torus Hall, and the comparison of measured and calculated neutron fluence was derived. Important lessons were learnt from this first experiment, which led to significant improvements in the experimental arrangements to reduce the effects of uncertainty due to directional neutron source and shielding interference of TLDs. These measurements have been carried out in preparation of full experiments to be performed during the planned DT operations with 14 MeV neutrons.

We report here the second series of measurements carried out during the 2013-2014 JET campaigns, and the related analyses. As in the previous experiment, the LiF:Mg,Cu,P TLD detectors have been developed and produced at the IFJ in Kraków. These detectors were located in the 2012 locations and in five additional positions, at larger distances from the plasma source in the SW labyrinth and in the basement below the SE chimney (see Figs. 1 - 4). The SW labyrinth is a 5-segment dogleg accessing the Torus Hall, with a side wall reinforced with borated concrete. In the chimney area, three large air ducts penetrate through the Torus Hall floor down to the basement and from there extend in different directions. In this experiment we concentrated on the duct which extends towards the south trench as shown in Fig. 4.

Numerical simulations were carried out to calculate neutron fluence and air kerma from neutrons using the MCNP code and a validated geometrical model of JET. In general, in the analyses performed to produce distributions of neutron fluence in large plant areas, far from the neutron source and with sufficient statistical accuracy, different approaches can be used. The track length estimator of particle flux (which provides the average flux over a defined volume) can be used to calculate the flux in given volumes in multiple step runs using the Surface Source Write /Read capability available in MCNP: at each separate run the neutron angular flux is recorded onto a surface from which they are initiated again in a new run and transported further in a region closer to the volumes of interest. Alternatively, the mesh tally capabilities of MCNP can be used to produce spatial maps of neutron fluence in the defined volume. In the mesh tally, a geometry independent 3-D tally grid is used to calculate volume averaged fluxes for each voxel in that grid. Extensive use of the variance reduction technique is needed in order to achieve sufficient statistical accuracy. In the analysis of this experiment, these different approaches were used and compared. Neutron cross section data were taken from the Fusion Evaluated Neutron Data Library (FENDL-2.1) [7], which is the reference neutron cross section library for ITER.

The calculated neutron fluence and air kerma at TLD positions were finally compared with the experimental results. The effect of the PE moderator and the TLDs shielding interference effect

was analysed as well. In addition, sensitivity analysis was performed to evaluate the effect on the calculated fluence due to variation of hydrogen and boron content in the concrete.

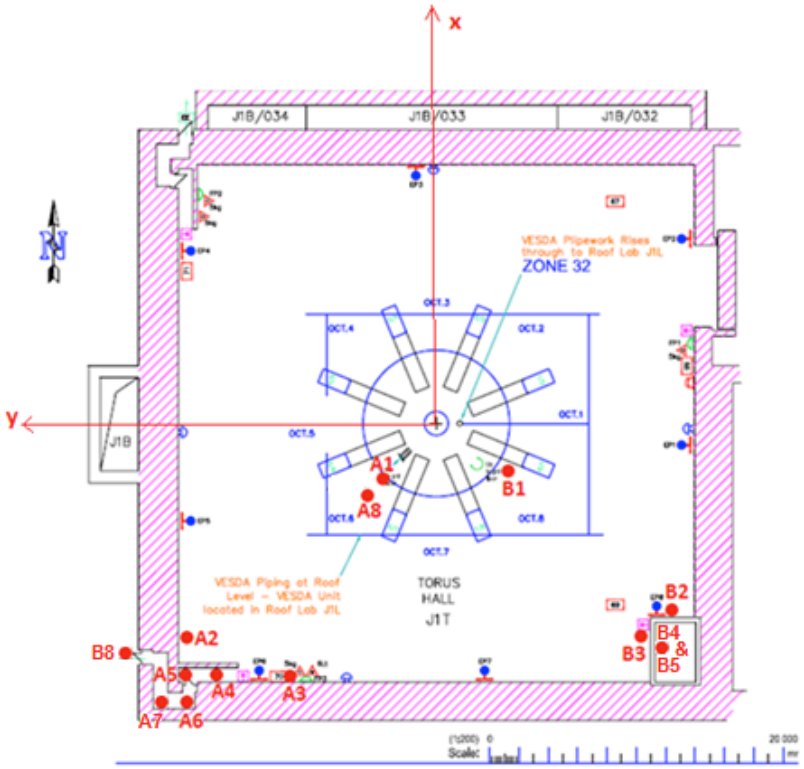

Fig. 1. Overview of TLDs location areas in the JET Torus Hall. Note that detectors are at different heights (see text).

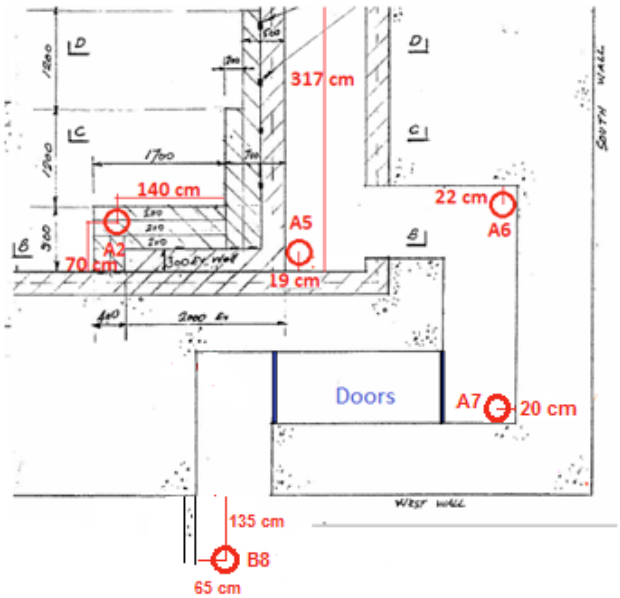

Fig.2. TL detectors in the SW labyrinth area. Detectors are at different heights (see text).

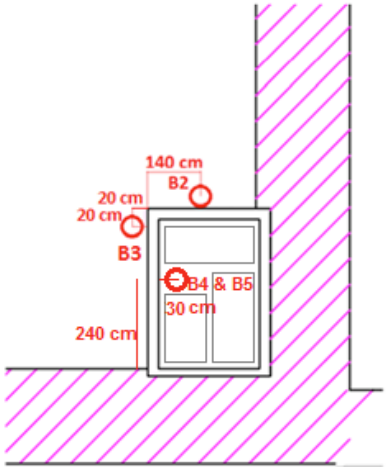

Fig.3. TL detectors in the SE chimney. The three rectangles inside the chimney are the air ducts penetrations through the Torus Hall floor. Detectors are at different heights (see text).

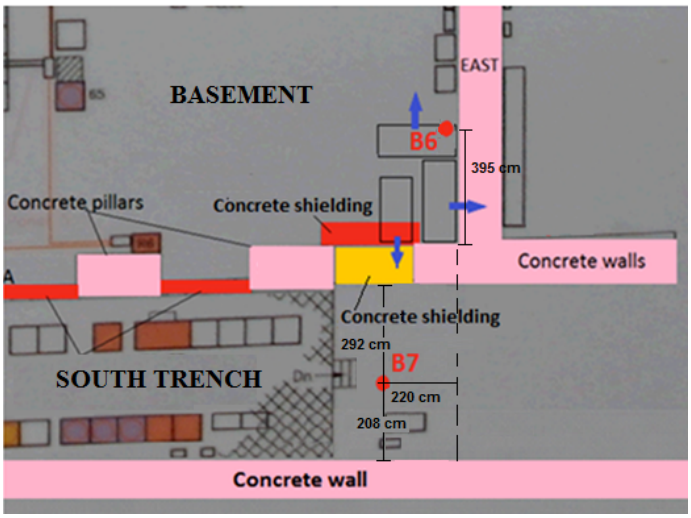

Fig.4. TL detectors in the basement – below the chimney area. The projection of the air ducts is also shown with indication of their direction from the basement (blue arrows).

2. Experimental set up

2.1 Characteristics of TL detectors and preparation for measurements

Several hundreds of lithium fluoride detectors of two types, made by the sintering technique, were manufactured at the Institute of Nuclear Physics (IFJ) in Krakow, annealed and prepared for measurements. Highly sensitive LiF:Mg,Cu,P (MCP-N) and ^{7}LiF:Mg,Cu,P (MCP-7) detectors were used, equivalent to TLD-100H and TLD-700H, respectively. ^{6}Li abundance in natural lithium is 7.59% while in ^{6}Li-suppressed lithium the residual ^{6}Li amounts to 0.03%.

Due to the large difference in the ^{6}Li and ^{7}Li isotopes' neutron capture cross sections (see Fig. 5), using pairs of ^{nat}LiF and ^{7}LiF detectors allows one to distinguish between neutron/non-neutron components of radiation field: LiF detectors with natural lithium are highly sensitive to slow neutrons, their response to neutrons being due predominantly to ^{6}Li lithium; on the other hand, LiF detectors consisting virtually entirely of ^{7}Li are almost insensitive to neutrons.

All MCP-N and MCP-7 detectors used had 4.5 mm diameter and 0.9 mm thickness, and were polished on both sides. The detection threshold of highly sensitive MCP detectors is below 1 μGy. The linearity range for this material extends to the level of a few Gy, whilst the saturation dose is about 1 kGy. However, due to the recently discovered MCPs' high-dose high-temperature emission they are able to measure doses up to 1 MGy [4]. All TLDs were prepared by a standard pre-irradiation annealing cycle (two-phase heat treatment): 260°C for 10 minutes followed by 240°C for 10 minutes. Then, all detectors were irradiated with the same dose of 10 mGy and readout using an automatic TL reader. In this way, individual response factors were derived for each detector. The TL signals measured for all detectors were calibrated in terms of kerma in air with ^{137}Cs gamma rays. For gamma rays, it can be demonstrated that kerma in air is equivalent to dose in air under the charged particle equilibrium conditions provided by the PE boxes. Finally, the pre-irradiation annealing procedure was applied for a second time in order to prepare the TLDs for the measurement campaign.

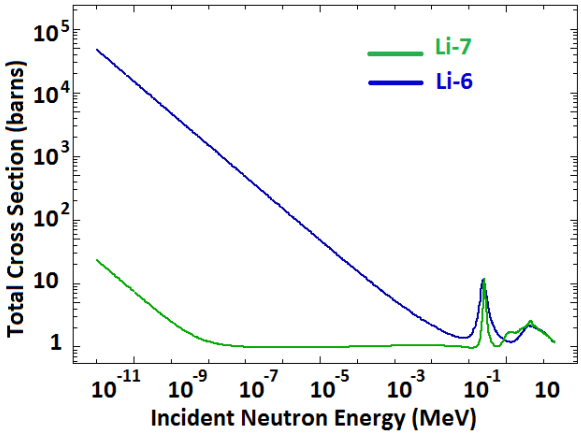

Fig.5. Total neutron cross sections of ^{6}Li and of ^{7}Li

2.2 Arrangement of TLDs in polyethylene moderators

In order to enhance the sensitivity to neutrons, all TLDs were located in the centre of cylindrical moderators made of high density polyethylene PE-HD (PE-300) (Fig. 6). Each moderator consisted of moderator body (cylinder) and a plug (30 mm diameter) with detector's boxes mounted at the bottom of it. The diameter of cylinders was in the range 25.0-25.5 cm, whilst the height was either 21 cm or 25 cm. TLDs were located in the cylinder centres in two types of PE-HD boxes, each with 6 mm thickness: circular boxes screwed in horizontal orientation at the bottom of the plug, and rectangular boxes inserted in vertical slots in the plugs at a minimum distance above the screw. This new arrangement in the 2013-2014 campaign was adopted in order to detect any effect due the directional flux of neutrons. In fact, TLDs located upstream, especially the MCP-N ones which contain a higher amount of ^{6}Li, can cause a shadowing effect on those located downstream. Photographs of the detector's boxes and moderator's plug without boxes and with boxes mounted are presented in Figure 6.

Moreover, in order to reduce the interference between TLDs containing ^{6}Li, due to self-shielding, and the shadow effect in the directional neutron flux, it was decided to reduce the number of TLD types used in the previous 2012 campaign in each single position [5]: the ^{6}LiF:Mg,Cu,P detectors (MCP-6) were excluded because they presented a large self-shielding effect, and the LiF:Mg,Ti (MTS) were excluded because they have a lower sensitivity. The total number of TLDs in each position was then reduced to 10, five MCP-N and five MCP-7 in each box (see Fig. 7).

Two circular and one rectangular boxes were prepared for background measurement (BG1-3). Some TLDs of each type were packed in polymethacrylate (PMMA) boxes and kept in low dose lead container/house at IFJ laboratory for calibration purposes and background evaluation.

Fig. 6. Left top: The PE-HD boxes with TLDs in place. Left bottom: Some of the plugs with detectors' boxes mounted. Right: The Cylindrical Polyethylene moderator.

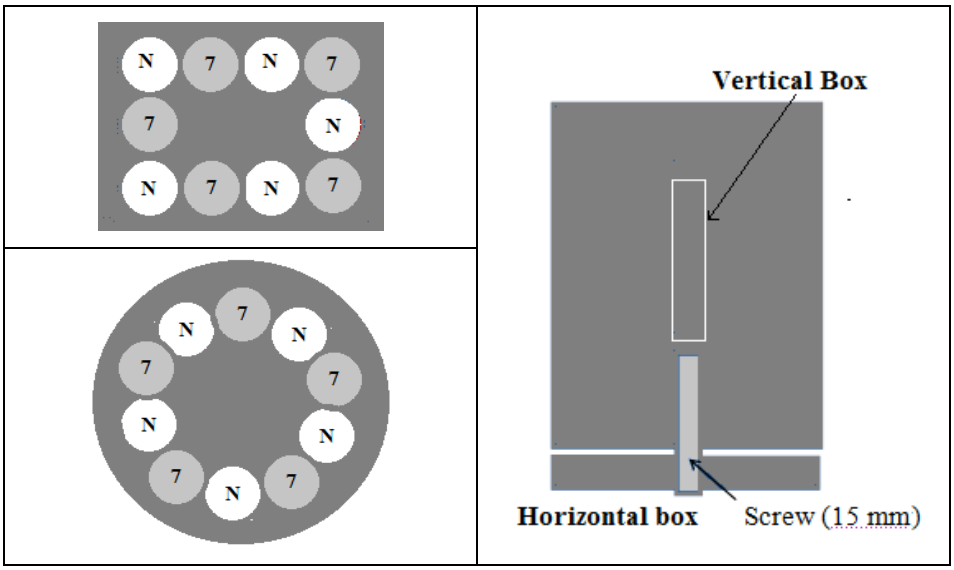

Fig. 7. Left: TLDs arrangement in the horizontal (circular) detectors' box screwed at the plug bottom and the vertical (rectangular) box inserted in a vertical slot in the plug. "7" indicates MCP-7 and "N" indicated MCP-N detectors. Right: The horizontal and vertical boxes in position in the plug.

2.3 Measurement campaigns at JET

All dosemeters arrived at Culham in June 2013 and were installed at JET on Sunday, 22 September 2013. Some dosemeters were located within their boxes in an office drawer for background measurement. Due to an unplanned interruption of JET experimental campaign, all dosemeters were removed on 11 October after 2 weeks of exposure at JET during which the total

neutron production was $2.76 \cdot 10^{18}$ neutrons[1]. New dosimeters were exposed again in the most distant positions (A6, A7, B8 and B6, B7 as well as B2 as reference position) when the campaign re-started, from 22 June to 6 September 2014. In this period, the total neutron yield was $9.90 \cdot 10^{18}$ neutrons.

Detectors A1, A8 and B1 were situated close to the tokamak, A2, A3, A4, A5, A6, A7 and B8 in the SW labyrinth area, B2, B3, B4 and B5 in the SE chimney corner, B6 in the basement below the chimney area and B7 in the south trench adjacent to the basement at about 60 m distance from the tokamak, see Fig. 1-4. In the labyrinth area the TLDs were located at different heights varying between 190 cm and 337 cm. B2, B3, B4 and B5 were located at 203 cm, 530 cm, 580 cm and 12.5 cm from the Torus Hall floor, respectively. B6 was at 190 cm height in the basement below the chimney area, and B7 on the horizontal duct at 407 cm height in the south trench. Finally, three dosemeters, BG1, BG2 and BG3 were located within their boxes in an office drawer for background measurement.

After each exposure period, all detectors were immediately sent back to the IFJ (Kraków, Poland) and read out using a Harshaw 3500 TL reader. They were annealed at 100°C for 10 minutes, then readout in a nitrogen atmosphere (140 l/h flow) with rate 2°C/s in the temperature range 100-270°C.

3. Experimental results

3.1 Results derived as mean value of the same type detectors' response

Results of TLDs measurements taken at the different positions are presented in Fig.8 as derived as mean values of the signal of MCP detectors of the same type (five detectors) at each position. The total uncertainty of measurements, including the uncertainty of detectors readout and the uncertainty of the ^{137}Cs gamma calibration, is ≈1% in all cases.

It can be seen that the measured doses decrease with distance from the plasma source, the variation spans about 4 orders of magnitude, from about 1 Gy down to 0.1 mGy in the areas investigated in the 2013 campaign. However, differences are observed locally due to the presence of massive apparatuses located in between the TLD positions and the closest tokamak main horizontal ports, the principal escaping paths for neutrons produced inside. For example, although B2 and B3 are located at the same distance from the tokamak, the measured dose at B2 is lower by a factor of about 2 because B2 is shielded by the Neutral Beam Injector located on the right hand side of the main horizontal port in Octant 8. Air kerma values are up to a factor of ten higher in MCP-N than in MCP-7 TLDs because of the neutron sensitivity of MCP-N detectors. However, at positions B8 (at the exit of the SW labyrinth) and B7 (on the horizontal duct in the South Trench in the SE chimney area) the differences in doses absorbed by MCP-N and MCP-7 are very small and they both approach the values registered by three background dosemeters. The office background registered is at the level of 0.2 mGy during the whole 2013 period between annealing and readout of the dosemeters (about five months) and is lower than the natural radiation background in Poland which has been monitored for thirty years by the IFJ, and is at the level of 0.2 mGy per quarter of year.

The new measurements performed in 2014 show that the air kerma values measured in B2, A6 and B6 are in very good agreement with the 2013 values when account is taken of the larger neutron yield in the 2014 campaign and after background subtraction. The integrated office background dose registered in the 2014 campaign is slightly lower than in 2013, but the dose rate is the same in the two measurement campaigns.

[1] Here the new JET neutron yield detector calibration obtained in 2013 has been applied

3.2. Calculation of neutron and non-neutron component of detectors response from measured values

LiF-based highly sensitive TL detectors present different responses to neutrons. In general, the response of the TLDs can be expressed as follows:

$$R_{tot}(7,N)_{MCP} = R_{\gamma} + R_n(7,N)_{MCP} \quad (1)$$

where R_{tot} is total response of detector of each type (7 or N), R_{γ} is its response to non-neutron part of the radiation field (in our case at JET mostly prompt gamma radiation), while R_n is its response to neutrons. The TLDs response $R_{tot}(7,N)_{MCP}$ were calibrated with gamma rays in terms of kerma in air $K_{tot}(7,N)$ which, in turn, can be expressed as:

$$K_{tot}(7,N) = K_{\gamma} + K_n(7,N) \quad (2)$$

where K_{γ} is the air kerma (gamma dose) due to gamma rays and K_n is air kerma due to neutrons. This second one depends not only on the type (7 or N) and material (MCP) but also on the geometry of the detector. As MCP-7 detectors contain only about 0.03% of ^{6}Li, it can be assumed in a first approximation that almost all their response is due to pure non-neutron component of the field of radiation, i.e. to gamma radiation in our case.

$$K_{tot}(7) \approx K_{\gamma} \quad (3)$$

Therefore, subtracting response of MCP-7 from the signal measured by MCP-N, it is possible to evaluate the TLDs response part due to the neutron component of the field. The resulting neutron dose for all positions is presented in Fig.9 for both the 2013 and 2014 measurements, together with total error calculated for each value (1σ). As the difference between MCP-N and MCP-7 are small in 2013 for A6, A7, B8, B6 and B7 due to the very low signals accumulated in only two weeks of operations, the derived neutron dose values are affected by large errors, shown in Fig.9 (±1σ). However, the new measurements obtained in 2014 are in very good agreement with those obtained in 2013 and are affected by smaller errors (Fig.9). The strong reduction in the experimental errors in 2014 measurements was due not only to the larger TL signals recorded during the campaign but also to the fact that all individual sensitivity factors were applied for each BG detector, and therefore a much smaller spread of results was obtained for the detectors in ach box. These results show that the neutron fluence is effectively attenuated through the SW labyrinth and down to the basement by about 6 orders of magnitude.

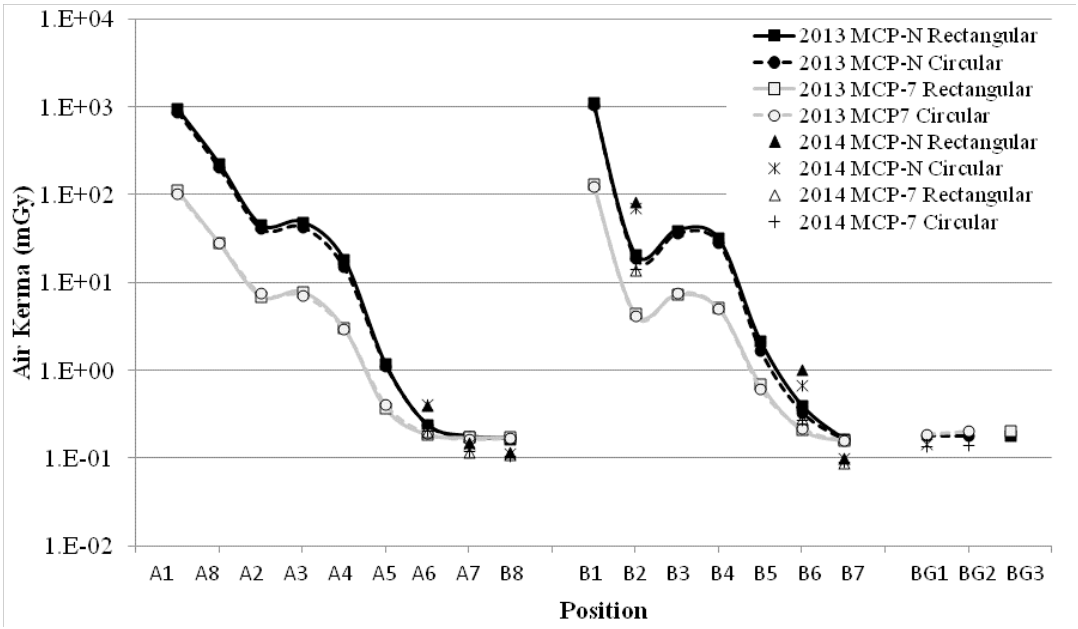

Fig. 8.Air kerma measured by MCP-N and MCP-7 detectors' response. For both MCP-7 and MCP-N detectors the mean value of all detector doses measured at each position is shown.

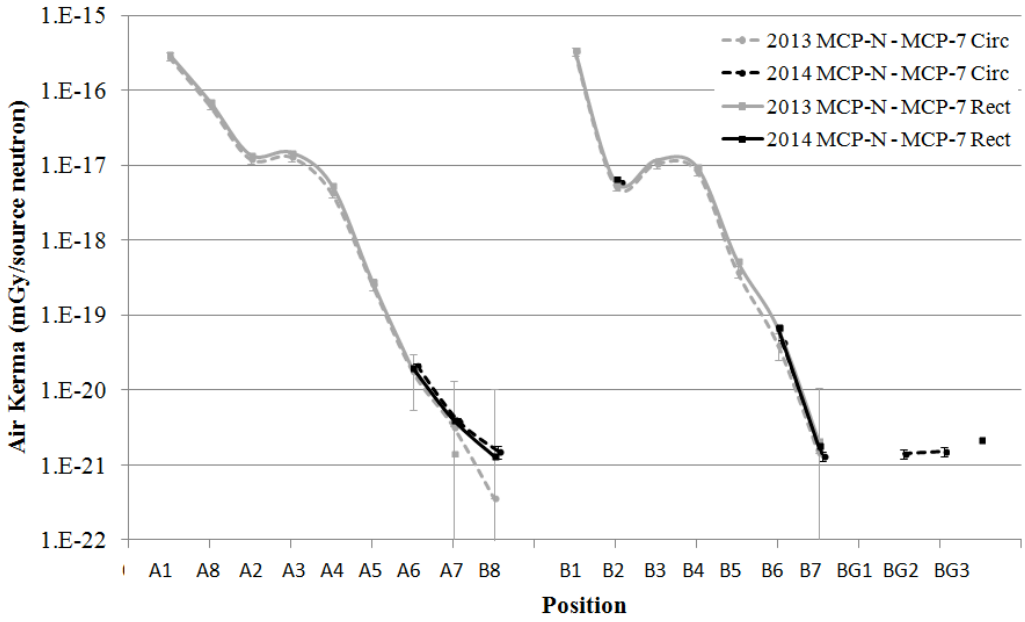

Fig. 9. Neutron air kerma per neutron source derived from response of MCP-N and MCP-7 detector types with different ^{6}Li content. Uncertainties are shown for all data (1σ).

3.3 Evaluation of neutron fluence

The response of TLDs due to the neutron components has been related to the local neutron fluence using the LiF detectors' calibration performed in 2006 by Burgkhardt et al. [8] at the PTB Thermal Neutron Reference Field at GeNF [7], and using the following definitions:

$$K_{tot}(7) = K_{\gamma} + \alpha_{7}\Phi_{n} \qquad (4)$$

$$K_{tot}(N) = K_{\gamma} + \alpha_{N}\Phi_{n} \qquad (5)$$

$$K_{tot}(N) - K_{tot}(7) = \alpha_N \Phi_n - \alpha_7 \Phi_n \qquad (6)$$

$$\Phi_n = \frac{K_{tot}(N) - K_{tot}(7)}{\alpha_N - \alpha_7} \qquad (7)$$

where Φ_n is the local neutron fluence at TLD position and $\alpha_{N,7}$ are coefficients (specific also for material used). Responses of LiF:Mg,Cu,P detectors of different types irradiated in a pure thermal neutron field were measured and the values resulted for MCP-N and MCP-7 detectors are presented in Table 1. It can be noted that the response of MCP-7 detectors to neutrons is much smaller than for MCP-N detectors' type, although not zero.

The gamma dose rate was also measured at the same PTB Thermal Neutron Reference Field with a commercially available instrument (FAG FH 40F2) behind a ^{6}LiF containing plate which fully stopped the neutron beam without gamma production. With gamma dose rate of about 2 μSv/h measured at the reference position, the ratio of gamma dose to neutron ambient dose equivalent was about $6 \cdot 10^{-4}$ and is therefore a negligible contribution [6].
Using the Burgkhardt calibration cofficients, the neutron fluence from kerma in air signal of detectors of each type can be derived at every measurement location. In fact, in the case of JET measurements, although the neutron spectrum is not thermal in any position in the Torus Hall, the large PE moderators ensures that the enclosed TLDs "see" a thermalized neutron field, and hence the Burgkhardt calibration factors can be applied. This assumption is discussed later with the experiment analysis (see §4.1). The results of this evaluation are presented in Fig. 10.

Table 1. Composition and dimensions of the different TLD used in this study and their related experimentally determined thermal neutron responses by Burgkhardt et al. [8].

Detector	Material	Size [mm]	Thickness [mm]	α Response to 1 n/cm^2 [mGy]	Standard uncertainty	
					u_{meas}[%]	u_{total} [%]
MCP-N	^{nat}LiF:Mg,Cu,P	Ø 4.5	0.9	4.10E-08	1.5	5.2
MCP-7	^{7}LiF:Mg,Cu,P	Ø 4.5	0.9	1.30E-09	1.2	5.1

The neutron fluence is about 10^{-8} n/cm^2/source neutron in positions A1 and B1 close to the machine and decreases by more than six orders of magnitude with increasing distance from the tokamak. It is worth stressing that these neutron measurements were only possible thanks to the use of the very sensitive TLDs.

It was also observed that the neutron component of the radiation field registered by detectors in rectangular boxes at each measurement position is systematically higher than registered by detectors in circular boxes (on average by about 19%). This difference could be attributed to the effect of directional flux for detectors A1-A7, B8 and B1-B4 for which the vertical box normal was always directed towards the machine centre, and so no shadowing effect can be expected. The orientation of B5 cylinder could not be checked because of difficulty of positioning it at the bottom of the chimney in the torus hall. B6 was located in the basement vertically below the chimney and in its case it is more correct to assume that the horizontal box was directed towards the source of neutrons streaming down the chimney. In this case however, the vertical box may have shielded the horizontal box located below.

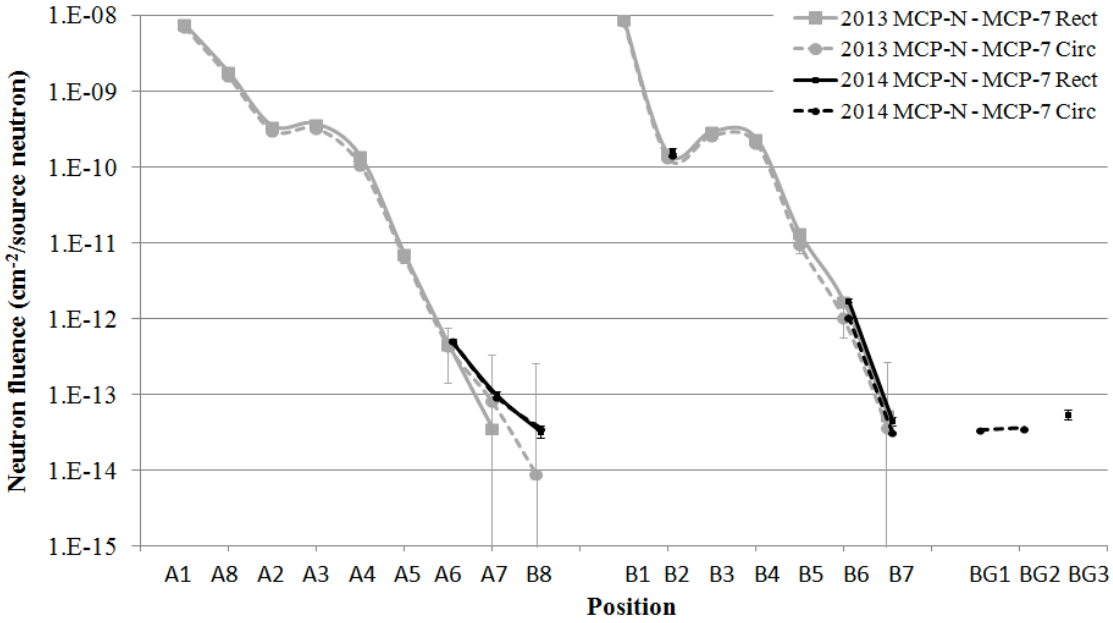

Fig. 10. Neutron fluence per JET source neutron at different positions evaluated from response of MCP-N and MCP-7 detector types with different Li-6 content using Burgkhardt calibration factors. Uncertainties are shown for all data (1σ).

4. Analysis of the experiment

The objective of numerical simulations is to calculate the neutron contribution to the air kerma and the neutron fluence at detectors and compare them with the measurements by TLDs. In all analyses, no attempt was made to calculate the fluence of prompt gamma rays and the related air kerma. Calculations have been carried out using the MCNP5-1.6/MCNPX-2.6 and MCNP-**6.1** [6], a validated geometrical model of JET and neutron cross-section data from FENDL-2.1 [7], which is the ITER reference nuclear data library. Two different approaches have been used as described below.

4.1. 2-step calculation method (C1)

In a first approach, the track length estimator has been used to calculate the neutron flux and the related air kerma for TLD detectors inside and outside the torus hall, with and without the polyethylene moderator in the positions where the TLDs would lie. The polythene cylinders were positioned as in reality, with TLD tally volumes modeled in detail. The detailed model of the JET torus includes the ITER-like Wall plasma facing components, the vacuum vessel, magnetic coils, shell, transformer limbs and concrete walls (Fig. 11a). Outside the shell and before the walls, however, there are numerous substantial structures which have not been modeled in detail. These are approximated with a thin zone surrounding the machine composed of iron, plastic and copper which has been adjusted in thickness to ensure that the measurements by the external neutron monitors (fission chambers) were consistent with the fluxes in the MCNP model. Although it is recognized that the thin zone approach is not an not ideal, the complexity in the torus hall is practically too high for more detailed modeling. The JET Torus Hall has been modeled without penetrations.

Moreover, for all detectors located outside the Torus Hall, a stage-by-stage simulation approach has been carried out, in which the detailed model of the JET was used to produce surface neutron sources: the Surface Source Write (SSW) / Surface Source Read (SSR) files capability in MCNP was used to register neutrons on two one-quarter spheres with centers at the SW hall

corner and the SE hall corner, respectively (1.0 m above the floor surface and radius of 5.0 m, see Fig.10a). The contribution of neutrons leaking from the torus and that are scattered in the wall materials was taken into account. The two SSW files were used as Surface Source Read (SSR) input file for the subsequent calculations for detectors in local regions in the labyrinth (Fig. 11b) and chimney areas.

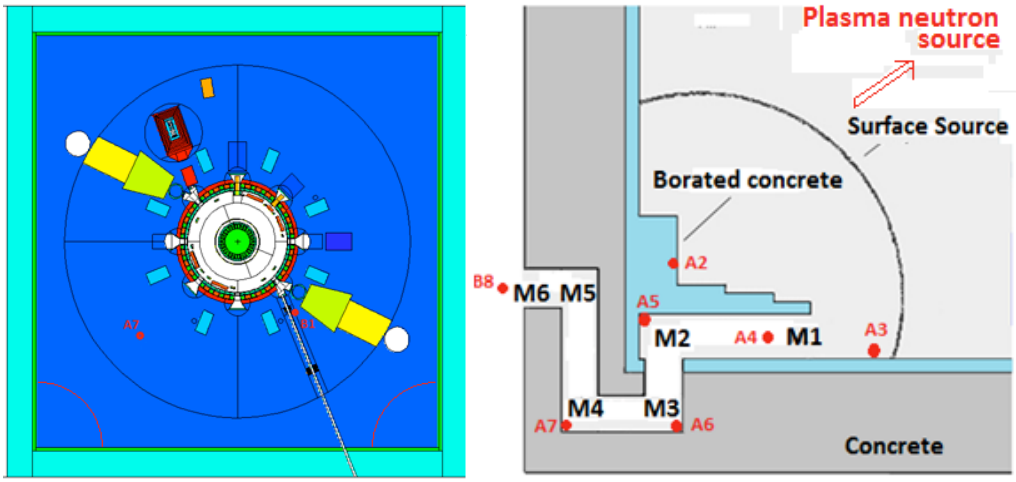

Fig. 11. a): MCNP model of JET - section at the machine midplane. Detectors B1 and A7 are visible as they are located close to the midplane (the others are at different heights). The SSW/SSR surfaces are shown in the SE and SW corners. See also Fig. 1 for comparison. b) Local MCNP model in the labyrinth area used for the second step calculation.

The evolution of the neutron fluence and energy spectrum along the SW labyrinth was investigated first using large spherical cells of 30 cm in radius, M1 - M6 in Fig. 11b, positioned at 100 cm height above the floor level. Position M1 corresponds to the inner entrance of the labyrinth (mouth) and position M6 to the JET Hall exit door. The labyrinth configuration includes four right-angle turns with a total length of 1180 cm, the height being 260 cm and the width 90 - 110 cm. The thickness of the concrete wall is 250 cm. The internal surface of the wall is covered by a layer of borated concrete (30 cm in thickness). The densities of concrete and borated concrete are 2.43 $g \cdot cm^{-3}$ and 2.20 $g \cdot cm^{-3}$, respectively. the composition is given in Table 2. Figure 12 shows the MCNP predicted neutron energy spectrum at positions M1-M6 for a D-D plasma source. The total neutron fluence calculated for the D-D plasma source is attenuated along the total length of the maze by about four orders of magnitude. The neutron fluence at the labyrinth exit was $(1.7 \pm 0.1) \times 10^{-13}$ cm^{-2} per JET neutron. Statistical uncertainties were < 10% (1σ) for all results, except one at the location near the labyrinth exit, which was ~15%.

It can be seen in Fig.12a that the fast neutrons produced in the tokamak and directed towards the labyrinth mouth have already been significantly down-scattered by the machine, the surrounding structures and wall materials and have lost a significant fraction of their kinetic energy. During their transport along the labyrinth, neutrons are elastically scattered in the labyrinth path direction by the wall materials and are further slowed down, but in all positions (in air) high energy tails are still present in the spectra, up to the keV region in M6. However, inside the PE moderators the neutron energy spectrum is essentially a thermal neutron spectrum due to the moderating action of Polyethylene, as shown in Fig.12b referring to position A5. These results confirm the LiF detectors' calibration in terms of neutron fluence by Burgkhardt, presented in §3.3, can be applied in the detectors positions outside the Torus Hall.

The neutron fluence has then been calculated at the detector positions in the PE moderators in the labyrinth and in the chimney area. The two different types of TLDs were modeled in detail (MCP-N and MCP-7). The TLDs were located in round and rectangular polyethylene (PE) boxes

at the centre of cylindrical PE moderators as shown in Figs. 13. All the calculated results in TLDs were obtained within 10% statistical uncertainty, except for A6 (±22%), A7 (±35%), B6 (±19%) and B7 (±85%). The calculated neutron fluence ratio with and without the PE moderator provided an estimate of the neutron attenuation within the moderator material at each experimental location, which ranged from 0.33±7.4% in A2 to 0.22±9% in A5, and from 0.34±8.8% in B3 to 0.25±7.2% in B5.

Table 2 Concrete compositions ("as-built")

Element or Isotope	Mass fraction (%)		Element or Isotope	Mass fraction (%)	
	Plain	Borated		Plain	Borated
Al	0.8	6.5	H	0.56	0.2
Ba	0.026	0.045	Fe-54	0.1508	0.174
B-10	0.0008	0.14	Fe-56	2.38472	2.752
B-11	0.0032	0.56	Fe-57	0.052	0.06
Ca	28	6.5	Fe-58	0.00728	0.0084
C	7.9	0.18	Mg	0.55	0.8
Cr-50	0.000129	0.000103	Mn	0.04	0.05
Cr-52	0.002514	0.002011	O	47.9	47.4
Cr-53	0.000285	0.000228	K	0.3	1.4
Cr-54	0.0000709	0.000057	Si	12	29.6
Co	0.00066	0.0008	Na	0.035	1.6
Cu-63	0.0005533	0.001522	S	0.18	0.13
Cu-65	0.0002466	0.000678	Ti	0.035	0.45
Eu-151	0.0000239	0.000033	Th	0.00022	-
Eu-153	0.0000261	0.000037	Zn	0.003	-
Ga	0.0004	0.0016			

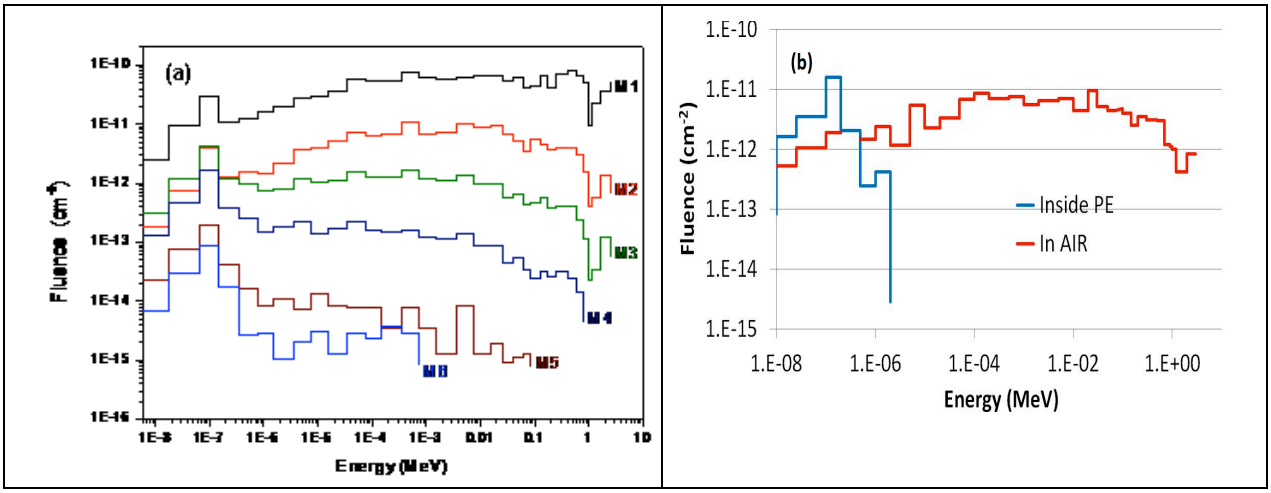

Fig. 12 a) Neutron energy spectrum in air at labyrinth positions M1-M6 for D-D plasma**. b)** Comparison of neutron spectra in air and in the centre of the PE moderator in position A5 in the labyrinth

Finally, the self-shielding effect and interference between TLDs were investigated via modelling: these effects cause perturbations in neutron fluence at the position of each individual TLD due to neutron absorption by all other TLDs (see Fig. 14a). The interfering shielding factors were calculated as the ratio of the neutron fluence in PE at the geometrical cell that would have been occupied by a single TLD with all other 19 TLDs present (Fig. 14) over the "unperturbed" neutron fluence in the same volume without TLDs. Separate factors were derived

(a (b (c)

for the round and the rectangular PE boxes for each detector type (MCP-N, MCP-7) and PE boxes configuration. The calculated interference shielding factors were in general low, in the range of 0.93 to 1.01, depending on the test volume position, thanks to the improved arrangement of TLDs in the boxes. For A2 position, this factor was within the range 0.93 – 0.98 and 0.96 – 1.00 for the MCP-7 and MCP-N type TLD, respectively. For B2 position, it was within 0.94 – 0.99 and 0.96 – 1.01 for the MCP-7 and MCP-N type TLDs, respectively. Moreover, in both positions they were lower for the horizontally oriented round boxes than those calculated for the vertically oriented rectangular boxes. These factors were used to correct the calculated air kerma and neutron fluence at TLD locations. It is important to point out here that the self-shielding correction for each TLD on itself was not applied as it was already taken into account in the calibration. In fact, the TLD is present when it is calibrated, and its signal is related to the known unperturbed neutron field in the TLD location.

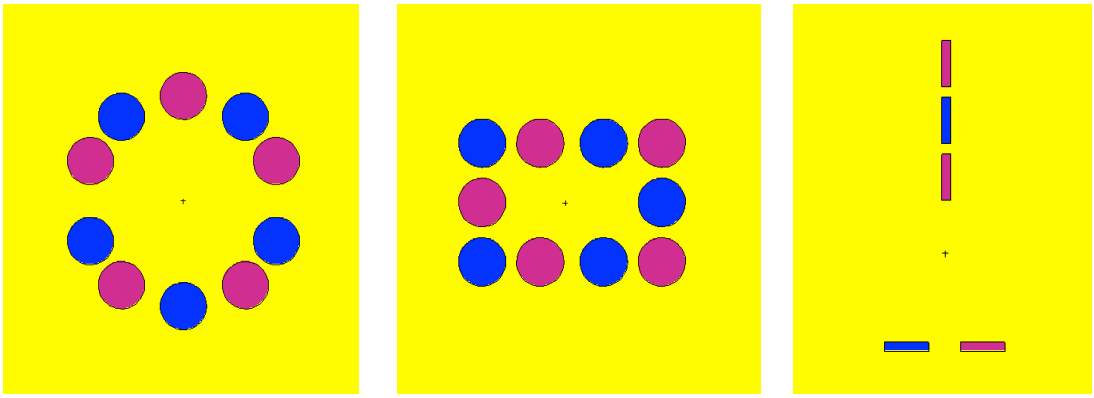

Fig. 13 MCNP models of the round box (a), the rectangular box (b) and the PE moderator including the two PE box (vertical cross-section)(c) Different colors indicate different types of TLDs.

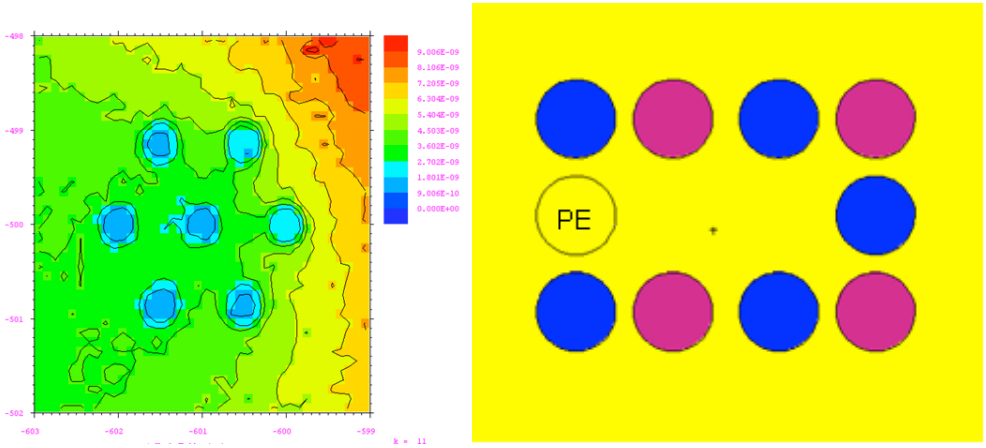

Fig. 14 a) Map of neutron flux inside Polyethylene cylinders with MCP-N TLDs only (configuration not adopted in the experiment), showing the self-shielding interfering effect and the shadowing effect between TLDs (the neutrons source is in the direction of the top right corner). b) Example of scoring region for interference shielding calculation modeling the real experimental configuration.

4.2. Mesh tally calculation method (C2)

In a second approach, the mesh tally capability has been used to calculate the neutron flux and the air kerma maps in the Torus Hall and in the adjacent areas of the Torus Building. To achieve statistically well-defined fluxes in the large mesh regions global variance reduction (GVR)

techniques were used. The CCFE code WWITER was used which iteratively construct a mesh-based weight window (WW), and sets the weight range based on previous flux values, as per the work of Cooper and Larsen method [10]. This capability is largely used in ITER neutronics calculations [11??]. In this approach the same JET machine model was used as in C1, but additional massive instruments were added in the Torus Hall such as the Octant 7 interferometer and steel walkways in front of Octant 6 and midway between Octant 8 and 1. In addition all the Torus Hall penetrations were added in the model (as part of the JET Operator effort in preparation of the DTE2), as shown in Fig.15. In the mesh tally, a geometry independent 3-D tally grid is used to calculate volume averaged fluxes for each voxel in that grid (Fig.16b). The mesh size was 25 cm in all directions, which was comparable with the size of the PE moderators and, at the same time, could provide results with good statistical accuracy. The local neutron energy and fluences at the PE cylinders were then used to derive the attenuation coefficients due to the PE moderators at each position, so that the neutron fluence and air kerma at TLDs could be obtained. The air kerma was calculated by multiplying the neutron fluence spectrum with the flux-to-air kerma conversion factor from ICRP-74 [12]. All the calculated results were obtained within 8% statistical uncertainty.The attenuation coefficients ranged from 0.81±7.2% in B1 to 0.37±8.9% in B6 for the fluence (slightly higher than found in C1), and from 0.088±8.2% in A1 to 0.062±8.2% in B6 for the air kerma. The interference shielding corrections were not calculated with this method, and not taken into account.

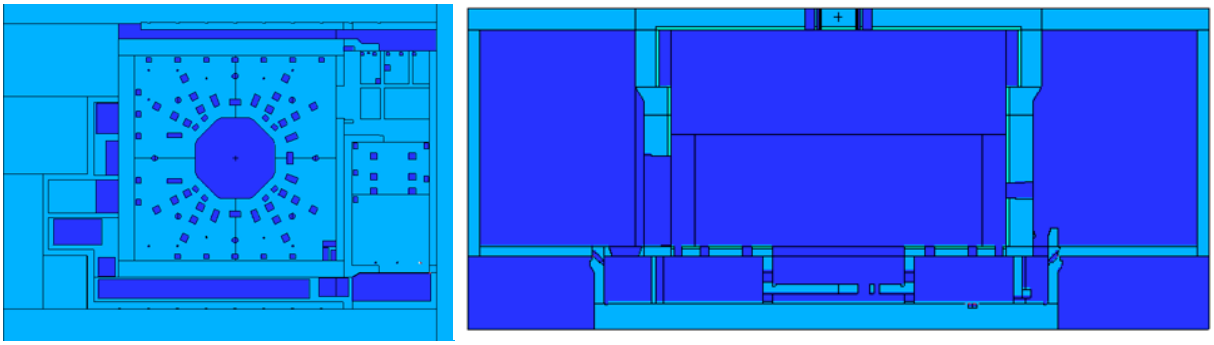

Fig.15 Improved MCNP model of JET to include penetrations of the Torus Hall. On the left: horizontal section of the floor; on the right: vertical section.

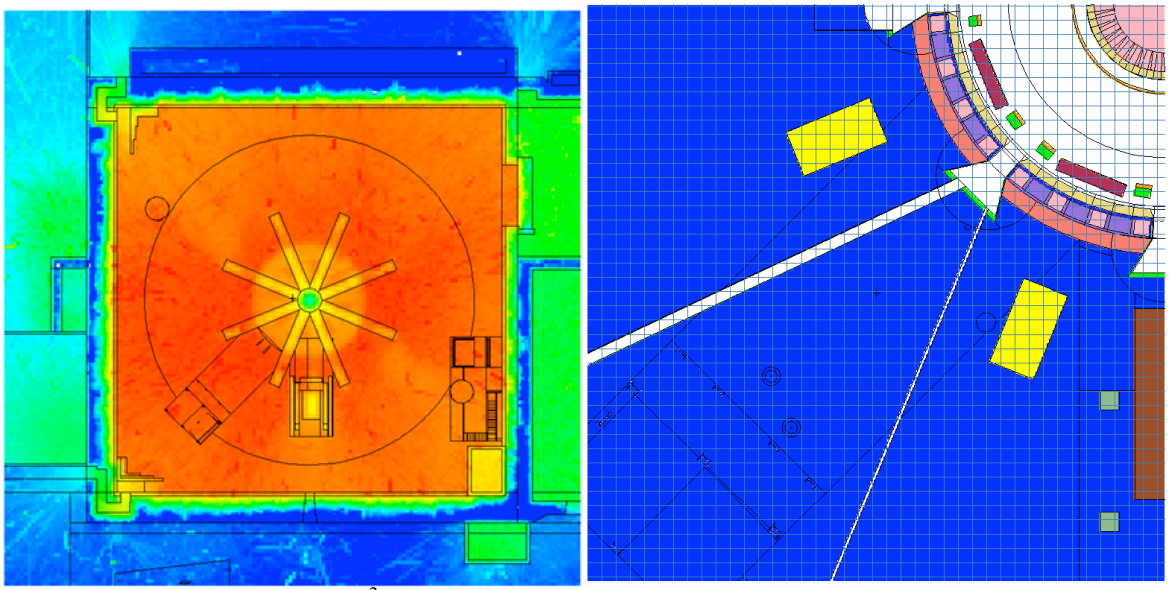

Fig.16 a) Neutron fluence map (cm-^{2}/source neutron) in JET Torus Hall, b) Image of the 25 cm independent 3-D tally grid over JET Geometry.

5. Results and Discussion

The comparison of calculated (C) over experimentally measured (E) neutron air kerma and neutron fluence values are given in Figs. 17 and 18, respectively, for TLDs located in horizontally oriented circular boxes. It should be noted that very similar results are found for those in vertically oriented rectangular boxes. As a general result, good agreement is found between C1 and C2 approaches, and between measurements and calculations over about 6 orders of magnitude variation. However, the agreement is lost for B7 and B8 positions for which the measured signal approaches the background level. Also, all calculations underestimate the measurements in A1, which is very close to the source in front of a port. It should be noted therefore that the uncertainty on the exact position of this detector, or the presence of a shielding equipment, would easily result in a large error.

The C/E ratios are shown in Fig. 19 for TLDs located in horizontally oriented circular boxes. Apart from A1, B7 and B8, very good agreement is found between calculations and measurements of the air kerma, while the neutron fluence is overestimated by both C1 and C2 methods. Howeover, several sources of uncertainties must take into account in the C/E comparison:

(a) Approximations in the calculation of the neutron fluence at detector positions: MCNP model of JET has been developed to calculate the neutron flux and fluence inside the machine and outside up to the magnetic limbs where calibrated neutron yield monitors are located. JET machine is described to sufficient details in the MCNP model but the large diagnostic systems, heating systems and various equipment surrounding the machine are not described in detail in the MCNP model. The neutron scattering/absorption occurring in the equipment materials is not therefore taken into account and this can explain the overestimation of the neutron fluence.

(b) The TLDs were calibrated in a thermal neutron spectrum. The neutron spectrum is not fully thermalized by the use of polyethylene cylinders in positions close to the tokamak. In these positions, TLDs experience a significant flux of 2.45 MeV neutrons and the TLDs calibration factors are therefore not correct in these positions.

(c) The hydrogen contents in concrete is not accurately known as hydrogen is present in water whose content in concrete can also vary in time. Hydrogen plays an important role in neutron streaming/attenuation in concrete since it is the major contributor in neutron slowing down by elastic scattering and, moreover, it is an absorber of slow neutrons. Also boron plays an important role due to its very high neutron capture cross section.

Sensitivity analysis has been performed by varying the H, B content in both ordinary and borated concrete compositions: an alteration the H mass fraction (w/w) from 0.51% to 0.61% in plain and from 0.15% to 0.25% in borated concrete resulted in a reduction of ambient dose equivalent at the labyrinth exit by a factor of ~1.5. An increase in boron in borated concrete from 0% to 1% (w/w) resulted in a reduction in dose at the exit of the labyrinth by a factor of 2. These results show that hydrogen and boron in concrete have a non negligible effect on the streaming of neutrons along the SW labyrinth and that the accuracy of the simulations depends on the knowledge of the concrete composition. Nevertheless, the uncertainty in the calculations associated to the uncertainty in H, B concentration in concrete can be assumed to be well within a factor of two at B8 and B7 positions.

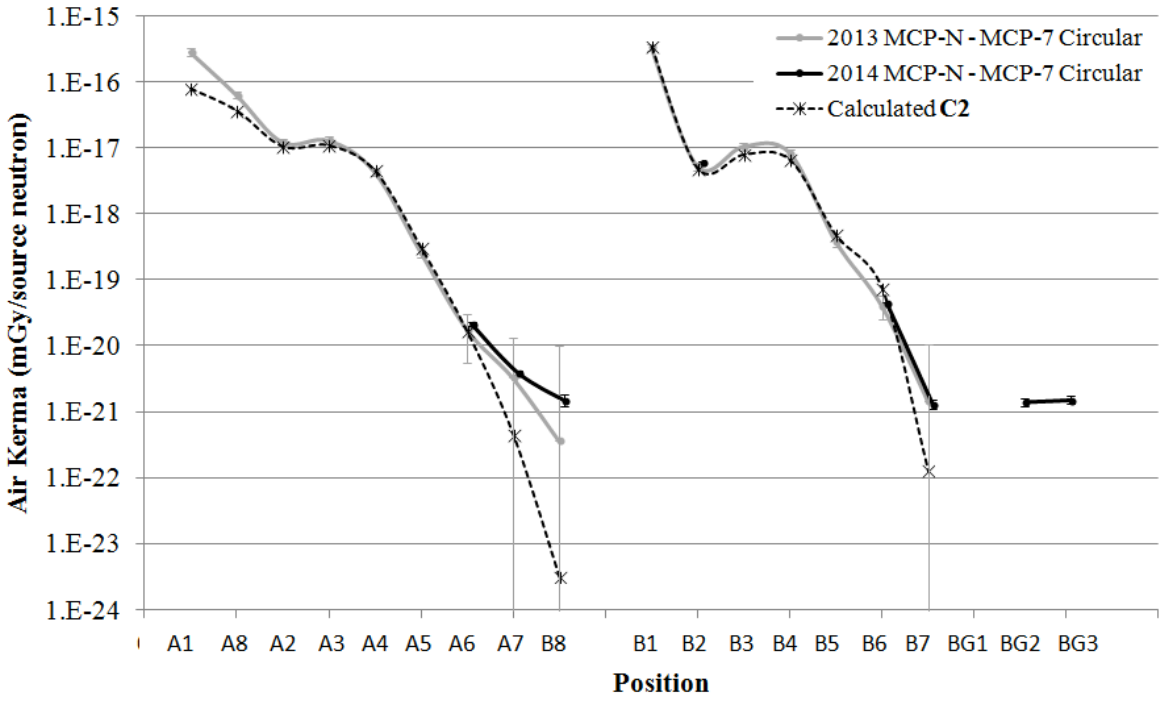

Fig. 17 Calculated and measured neutron air kerma for TLDs located in horizontally oriented circular boxes. Uncertainties are shown for all data (1σ).

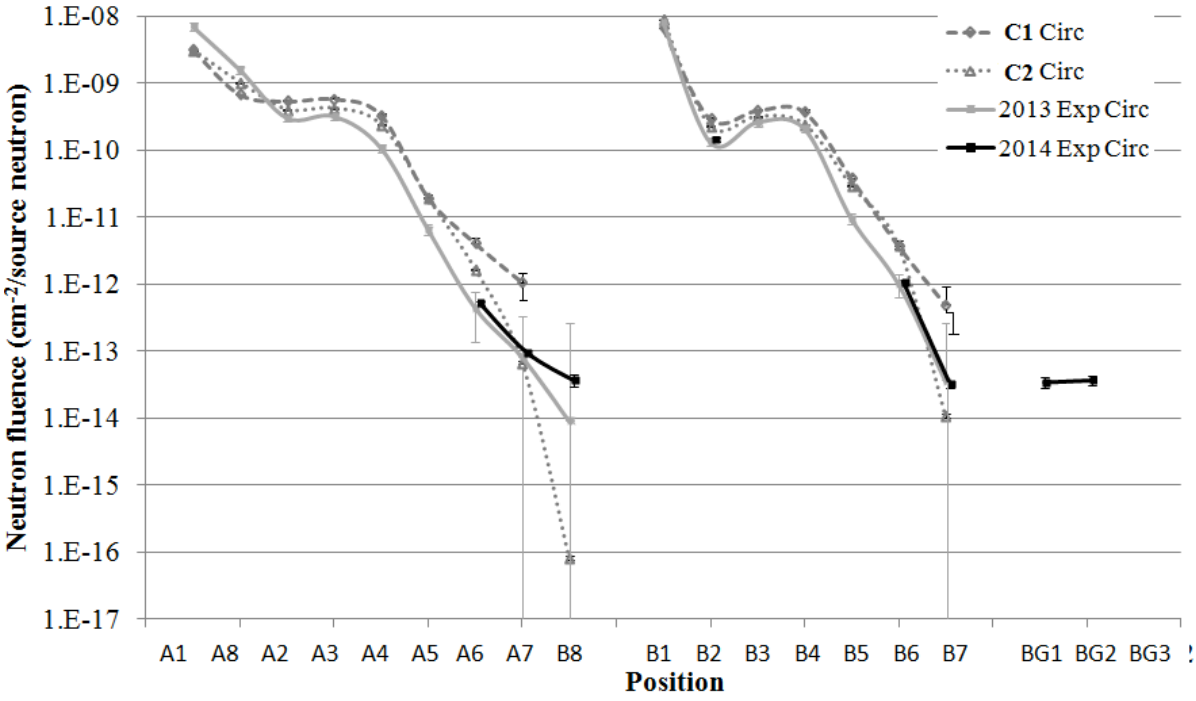

Fig. 18 Calculated and measured neutron fluence for TLDs located in horizontally oriented circular boxes. Uncertainties are shown for all data (1σ).

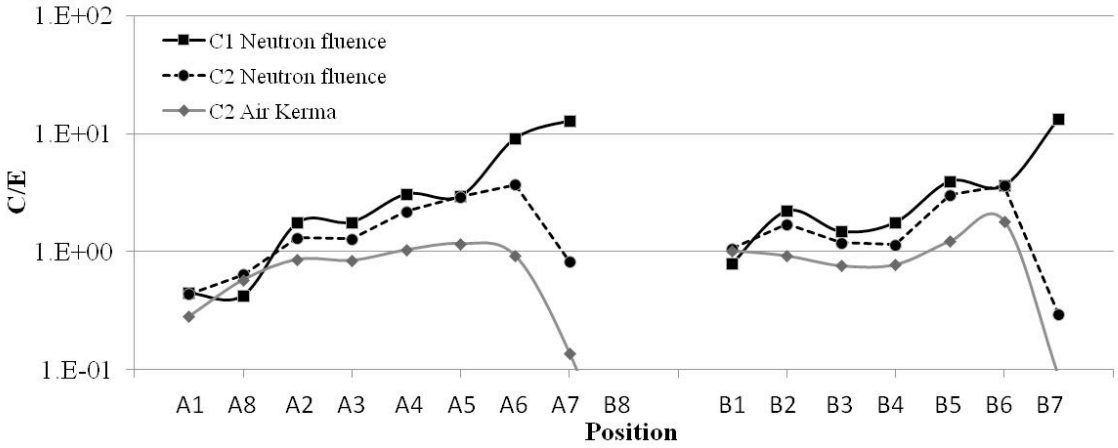

Fig.19 Ratios of Calculated (C) over measured (E) neutron air kerma for TLDs located in horizontally oriented circular boxes.

6. Conclusions

The neutron air kerma signal (dose in air) during JET plasma discharges has been measured in various positions close to the JET machine, at the Torus Hall walls, and outside the biological shield in the SW labyrinth and in the SE chimney down to the Torus Hall basement. The measurements were possible thanks to the use of two types of very sensitive TLDs: MCP-N and MCP-7. As these TLDs contain different amount of ^{6}Li and ^{7}Li, the different contributions of neutrons and of gamma rays to the total dose could be separated. Moreover, as the TLDs are also calibrated in terms of neutron fluence, the local neutron fluence could be obtained from the neutron dose measurements. The neutron fluence in the experimental positions varied over about six orders of magnitude, from about 10^{-8} n/cm^2/source neutron to 10^{-14} n/cm^2/source neutron. By the improvement of detector selection and positioning inside moderators it was possible to reduce the shielding interference between detectors, and the shadowing effect observed during the 2012 campaign for detectors containing ^{6}Li and this way to decrease the uncertainty of the measurement. These results confirm that the TLD technology can be usefully applied. During a JET campaign with substantial neutron production extensive mapping of the neutron fluence outside the JET biological shield can be obtained.

The results of MCNP simulations of the experiment have also been presented. The neutron contribution to the air kerma and the neutron fluence at detectors were calculated using neutron cross-section data from FENDL-2.1 with a validated geometrical model of JET. These calculations were compared with the measurements obtained using TLDs. Two different MCNP calculation approaches have been used, which are widely used in ITER analyses: a multiple step simulation approach making use of the Surface Source Write (SSW) Surface Source Read (SSR) files capability in MCNP and with track length estimator of the flux (C1), and the mesh tally track length estimator of the flux (C2).

The analyses of the experiment have shown that the PE moderators effectively thermalize the neutron flux at experimental positions outside the Torus Hall. The self-shielding interference between TLDs is strongly reduced in the improved detector arrangement to less than 7%, whilst the shadowing effect appears (by measurement) to be about 19% on average.

Apart from A1, B7 and B8, very good agreement is found between calculations and measurements of air kerma, whilst there appears to be a trend that is evident to overestimate C/E for neutron fluence with increasing distance by both C1 and C2. However, C/E << 1 are found in the most distant positions A7, B8 and B7, where the measured signal approaches the background level.

Other sources of uncertainties on the C/E comparison have been discussed, which are due to a) approximations in MCNP model of JET equipment present in the Torus Hall; (b) The not thermal neutron spectrum inside the PE cylinders in positions close to the tokamak; (c) the inaccurate knowledge of H, B contents in concrete, whose associated uncertainty has been quantified to be within a factor of 2 in the more distant positions.

These results provide a validation of neutronics calculations for ITER device and in the surrounding areas outside the ITER biological shield in relevant fusion conditions.

New improvements are planned at JET in view of repeating the measurements with 14 MeV neutrons during the DTE2. Measurements will be repeated again in the next DD campaign. The MCP-N and MCP-7 TLDs will be calibrated at 2.5 MeV and 14 MeV neutron energy, and with standard gamma sources. Moreover, the neutron fluence measured by TLDs will be complemented by activation foil based measurements using multiple foil technique in some positions inside the Torus Hall.

Finally, additional neutron streaming paths through the JET biological shield will be investigated, which are relevant both for JET DTE2 operations and for ITER.

Acknowledgement

This work has been started within EFDA and carried out within the framework of the and has received funding from the European Union's Horizon 2020 research and innovation programme under grant agreement number 633053. The views and opinions expressed herein do not necessarily reflect those of the European Commission.

References:

[1] P. Batistoni, J. Likonen, N. Bekris, S. Brezinsek, P. Coad, L. Horton, G. Matthews, M. Rubel, G. Sips, B. Syme, A. Widdowson, Fusion Engineering and Design, Volume 89, Issues 7–8, October 2014, Pages 896-900

[2] Bilski, P., 2002. Lithium Fluoride: From LiF:Mg,Ti to LiF:Mg,Cu,P. Radiat. Prot. Dosim. 100, 199-206.

[3] Obryk, B., Bilski, P., Budzanowski, M., Fuerstner, M., Glaser, M., Ilgner, C., Olko, P., Pajor, A., Stuglik, Z., 2009. Development of a method for passive measurement of radiation doses at ultra-high dose range. IEEE Trans. Nucl. Sci. 56, No. 6, 3759-3763.

[4] Obryk, B., Bilski, P., Olko, P., 2011. Method of thermoluminescent measurement of radiation doses from micrograys up to a megagray with a single LiF:Mg,Cu,P detector, Radiat. Prot. Dosim. 144, 543-547.

[5] B. Obryk, P. Batistoni, S. Conroy, B. D. Syme, S. Popovichev, I. E. Stamatelatos, T. Vasilopoulou, P. Bilski, Thermo-luminescence measurements of neutron streaming through JET Torus Hall ducts, Fusion Engineering and Design, Thermoluminescence measurements of neutron streaming through JET Torus Hall ducts, Volume 89, Issues 9–10, October 2014, Pages 2235-2240

[6] Initial MCNP6 Release Overview – MCNP6 version 1.0, J T Goorley et al, Los Alamos National Laboratory Report LA-UR-13-22934, Los Alamos, NM, US, 24th April 2013

[7] D. L. Adama, A. Trkov, FENDL-2.1 Evaluated nuclear data library for fusion applications, IAEA Report INDC (NDS)-467, Vienna, 2004

[8] Burgkhardt, B., Bilski, P., Budzanowski, M., Boettger, R., Eberhardt, K., Hampel, G., Olko, P. and Straubing, A., 2006. Application of different TL detectors for the photon Dosimetry in mixed radiation fields used for BNCT, Radiat. Prot. Dosim. 120, 83-86.

[9] Boettger, R., Friedrich, H., Janßen, H., 2004. The PTB Thermal Neutron Reference Field at GeNF, PTB-N-47, ISBN 3-86509-199-7.

[10] M.A. Cooper, E.W. Larsen, Automated Weight Windows for Global Monte Carlo Particle Transport Calculations, Nuclear Science and Engineering, 137, pp.1-13 (2001).

[11] A. Serikov, U. Fischer and D. Grosse, High Performance Parallel Monte Carlo Transport Computations for ITER Fusion Neutronics Applications, Progress in Nuclear Science and Technology, Vol. 2, pp.294-300 (2011)

[12] ICRP Publication 74, The 1996 Conversion Coefficients for use in Radiological Protection against External Radiation. ICRP 26 (3-4), 1996